Electronic Supplementary Information

The retrieving aromaticity of dithiadiazuliporphyrin by oxidation: Illustration by the experimental and theoretical investigation

Young Mo Sung,[a] Natasza Sprutta,[b] Jun Oh Kim,[a] Yun Hee Koo,[a] Lechosław Latos-Grażyński,[b,] and Dongho Kim[a,*]*

[a]Department of Chemistry, Yonsei University, Seoul 120-749, Korea, [b]Department of Chemistry, University of Wrocław, 14 F. Joliot-Curie Street, 50-383, Wrocław, Poland.

E-mail: dongho@yonsei.ac.kr, lechoslaw.latos-grazynski@chem.uni.wroc.pl

Contents

Figure S7. Calculated NICS(0) values and positions of monocation radical of dithiadiazuliporphyrin

Figure S8. Calculated NICS(0) values and positions of dication of dithiadiazuliporphyrin

Figure S9. The ACID plots of neutral dithiadiazuliporphyrin (isosurface valuce=0.05)

Figure S10. The ACID plots of monocation radical of dithiadiazuliporphyrin (isosurface valuce=0.05)

Figure S11. The ACID plots of dication of dithiadiazuliporphyrin (isosurface valuce=0.05)

Table S1. The HOMA, MPD, and NICS(0) value of a series of dithiadiazuliporphyrin

Table S2. TD-DFT (B3LYP/6-31G(d,p)) calculated energies, oscillator strengths and compositions of the major electronic transitions of neutral dithiadiazuliporphyrin

Table S3. TD-DFT (B3LYP/6-31G(d,p)) calculated energies, oscillator strengths and compositions of the major electronic transitions of monocation radical of dithiadiazuliporphyrin

Table S4. TD-DFT (B3LYP/6-31G(d,p)) calculated energies, oscillator strengths and compositions of the major electronic transitions of dication of dithiadiazuliporphyrin

1. Experimental Details

Steady-state Absorption Measurements. Steady-state absorption spectra were obtained with an UV-VIS-NIR spectrometer (Varian, Cary5000).

Femtosecond Transient Absorption Measurements. The femtosecond time-resolved transient absorption (fs-TA) spectrometer consisted of Optical Parametric Amplifiers (Palitra, Quantronix) pumped by a Ti:sapphire regenerative amplifier system (Integra-C, Quantronix) operating at 1 kHz repetition rate and an optical detection system. The generated OPA pulses had a pulse width of ~ 100 fs and an average power of 100 mW in the range 280-2700 nm which were used as pump pulses. White light continuum (WLC) probe pulses were generated using a sapphire window (3 mm of thickness) by focusing of small portion of the fundamental 800 nm pulses which was picked off by a quartz plate before entering to the OPA. The time delay between pump and probe beams was carefully controlled by making the pump beam travel along a variable optical delay (ILS250, Newport). Intensities of the spectrally dispersed WLC probe pulses are monitored by a High Speed spectrometer (Ultrafast Systems). To obtain the time-resolved transient absorption difference signal (DA) at a specific time, the pump pulses were chopped at 500 Hz and absorption spectra intensities were saved alternately with or without pump pulse. Typically, 4000 pulses excite samples to obtain the fs-TA spectra at a particular delay time. The polarization angle between pump and probe beam was set at the magic angle (54.7°) using a Glan-laser polarizer with a half-wave retarder in order to prevent polarization-dependent signals. Cross-correlation fwhm in pump-probe experiments was less than 200 fs and chirp of WLC probe pulses was measured to be 800 fs in the 400-800 nm region. To minimize chirp, all reflection optics in the probe beam path and the 2 mm path length of quartz cell were used. After the fluorescence and fs-TA experiments, we carefully checked absorption spectra of all compounds to detect if there were artifacts due to degradation and photo-oxidation of samples. HPLC grade solvents were used in all steady-state and time-resolved spectroscopic studies. The three-dimensional data sets of ΔA versus time and wavelength were subjected to singular value decomposition and global fitting to obtain the kinetic time constants and their associated spectra using Surface Xplorer software (Ultrafast Systems).

Computational Methods. Quantum mechanical calculations were performed with the Gaussian 09 program suite.[1] All calculations were carried out by the density functional theory (DFT) method with Becke's three-parameter hybrid exchange functionals and the Lee-Yang-Parr correlation functional (B3LYP), employing the 6-31G(d,p) basis set. The oscillator strength was calculated by performing a time dependent (TD)-DFT calculation.

Reference list

[1] *Gaussian 09, Revision A.1*, Frisch, M. J.; Trucks, G. W.; Schlegel, H. B.; Scuseria, G. E.; Robb, M. A.; Cheeseman, J. R.; Scalmani, G.; Barone, V.; Mennucci, B.; Petersson, G. A.; Nakatsuji, H.; Caricato, M.; Li, X.; Hratchian, H. P.; Izmaylov, A. F.; Bloino, J.; Zheng, G.; Sonnenberg, J. L.; Hada, M.; Ehara, M.; Toyota, K.; Fukuda, R.; Hasegawa, J.; Ishida, M.; Nakajima, T.; Honda, Y.; Kitao, O.; Nakai, H.; Vreven, T.; Montgomery, Jr., J. A.; Peralta, J. E.; Ogliaro, F.; Bearpark, M.; Heyd, J. J.; Brothers, E.; Kudin, K. N.; Staroverov, V. N.; Kobayashi, R.; Normand, J.; Raghavachari, K.; Rendell, A.; Burant, J. C.; Iyengar, S. S.; Tomasi, J.; Cossi, M.; Rega, N.; Millam, N. J.; Klene, M.; Knox, J. E.; Cross, J. B.; Bakken, V.; Adamo, C.; Jaramillo, J.; Gomperts, R.; Stratmann, R. E.; Yazyev, O.; Austin, A. J.; Cammi, R.; Pomelli, C.; Ochterski, J. W.; Martin, R. L.; Morokuma, K.; Zakrzewski, V. G.; Voth, G. A.; Salvador, P.; Dannenberg, J. J.; Dapprich, S.; Daniels, A. D.; Farkas, Ö.; Foresman, J. B.; Ortiz, J. V.; Cioslowski, J.; Fox, D. J. Gaussian, Inc., Wallingford CT, **2009**.

2. Supporting Information

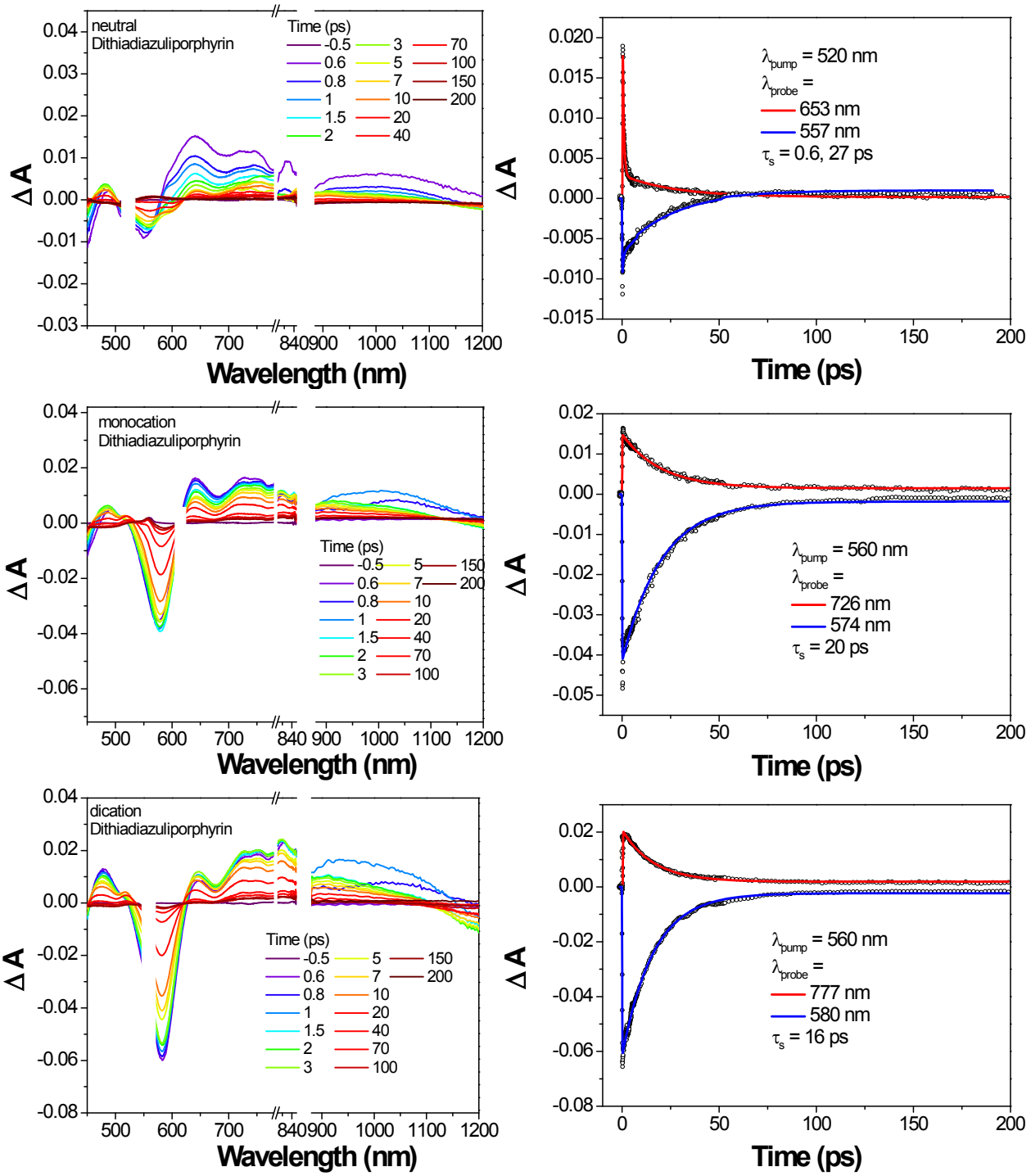

Figure S1. TA spectra (left) and decay profiles (right) of neutral (top), monocation radical (middle), and dication (bottom) of dithiadiazuliporphyrin

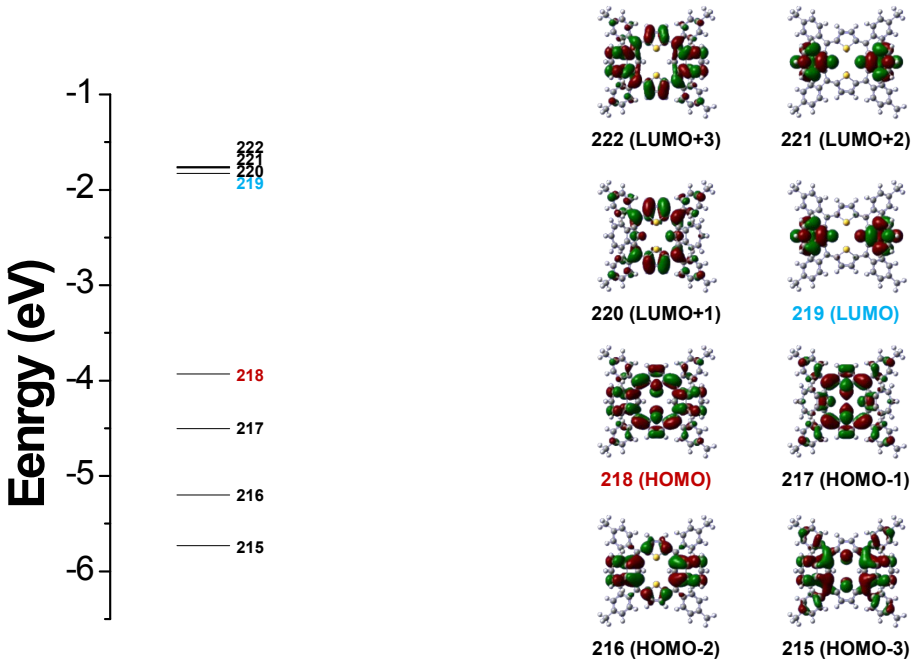

Figure S2. Calculated energy diagrams and MO of neutral dithiadiazuliporphyrin

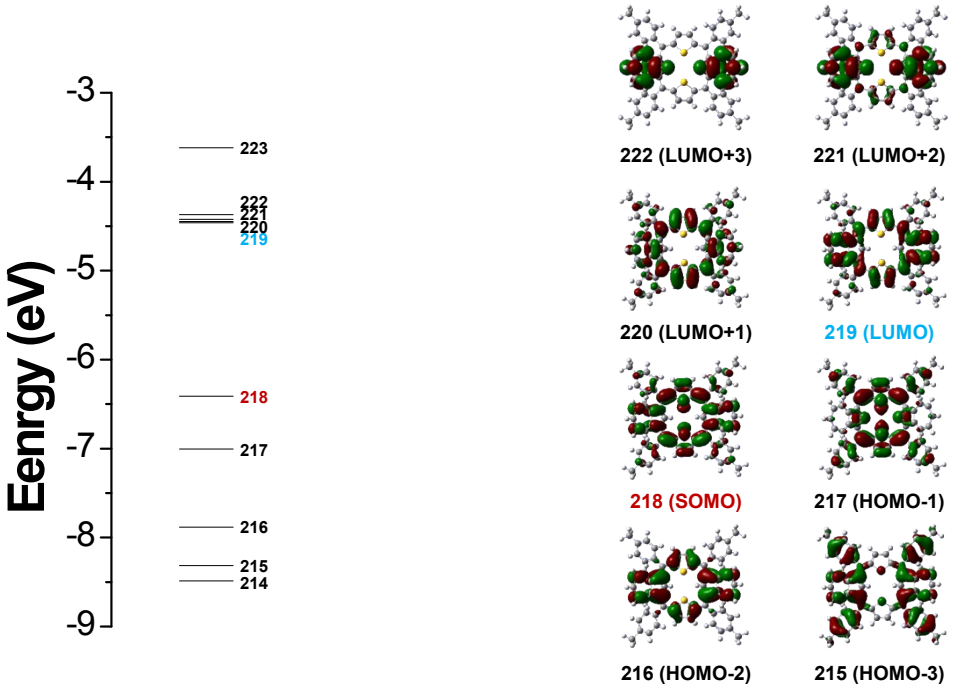

Figure S3. Calculated energy diagrams and MO of monocation radical of dithiadiazuliporphyrin

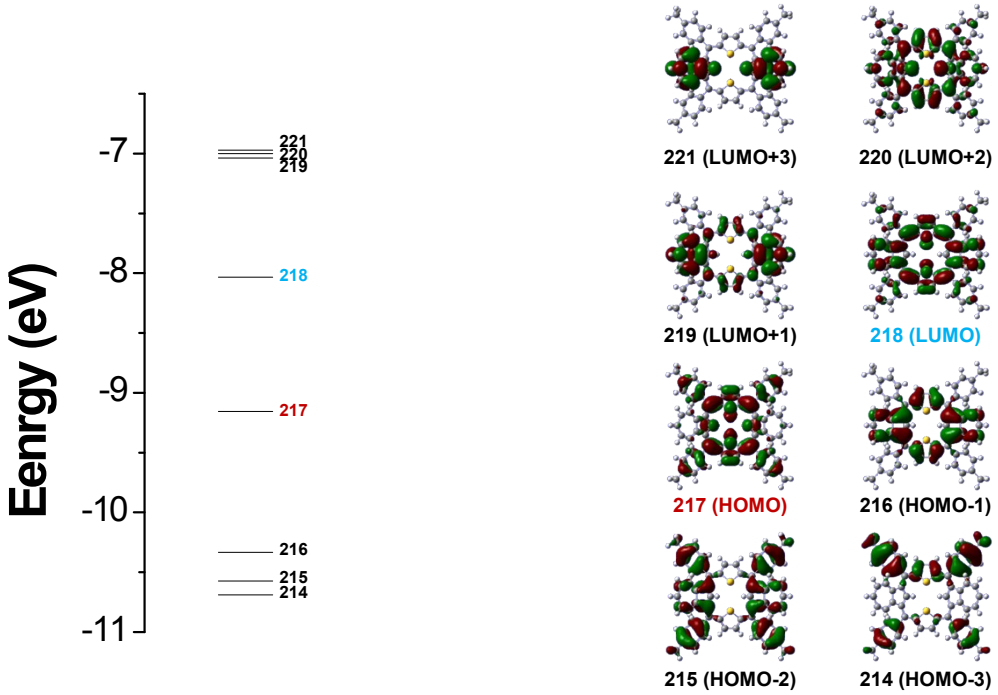

Figure S4. Calculated energy diagrams and MO of dication of dithiadiazuliporphyrin

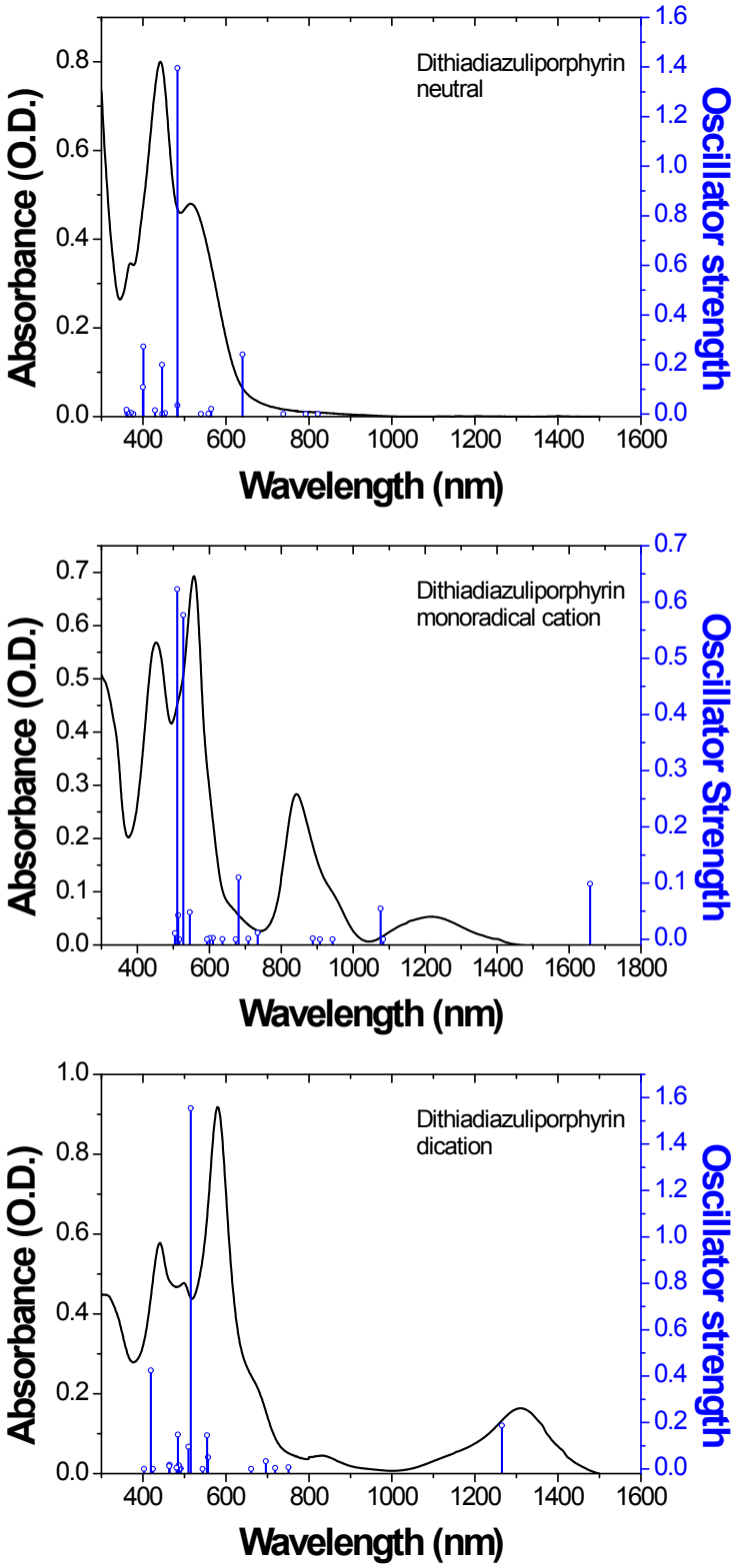

Figure S5. The absorption spectra with calculated vertical transitions of neutral (top), monocation radical (middle), and dication (bottom) of dithiadiazuliporphyrin

Neutral dithiadiazuliporphyrin

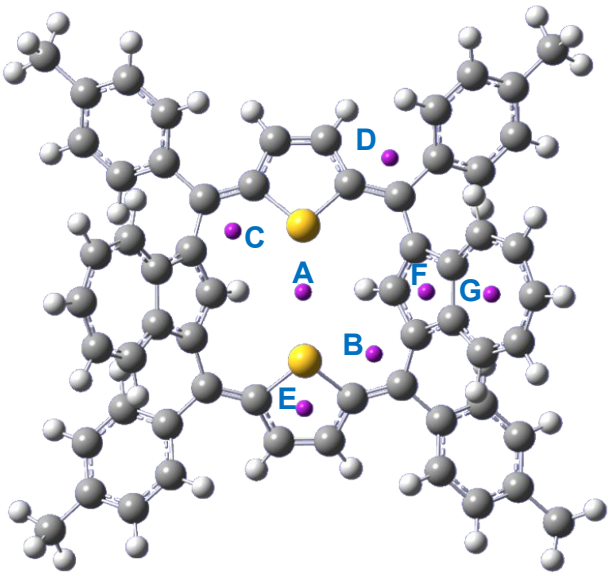

NICS(0) (ppm)
A: 0.415
B: 0.947
C: 0.942
D: -1.593
E: -2.897
F: -15.926
G: -4.730

Figure S6. Calculated NICS(0) values and positions of neutral dithiadiazuliporphyrin

Monocation radical of dithiadiazuliporphyrin

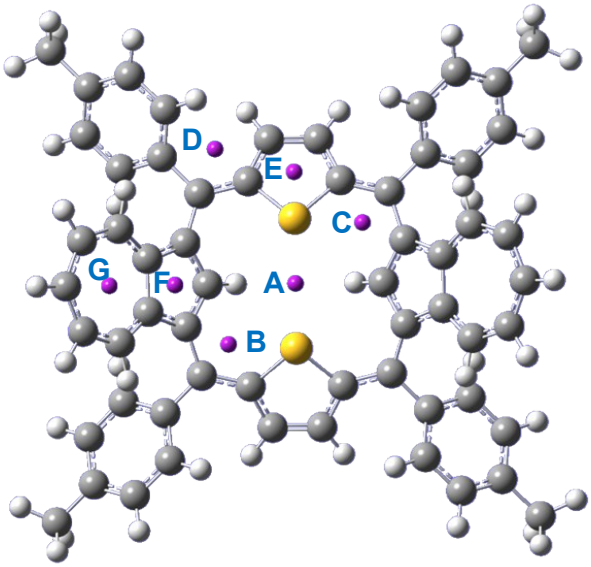

NICS(0) (ppm)
A: -2.881
B: -4.745
C: -4.745
D: 1.409
E: -7.119
F: -12.032
G: -3.153

Figure S7. Calculated NICS(0) values and positions of monocation radical of dithiadiazuliporphyrin

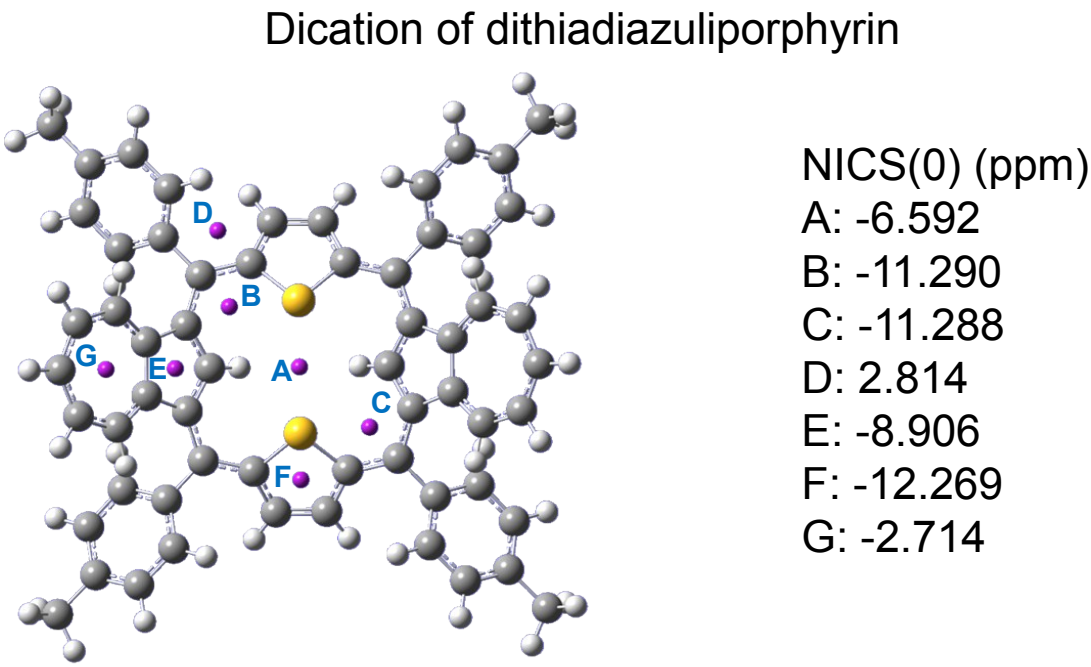

Figure S8. Calculated NICS(0) values and positions of dication of dithiadiazuliporphyrin

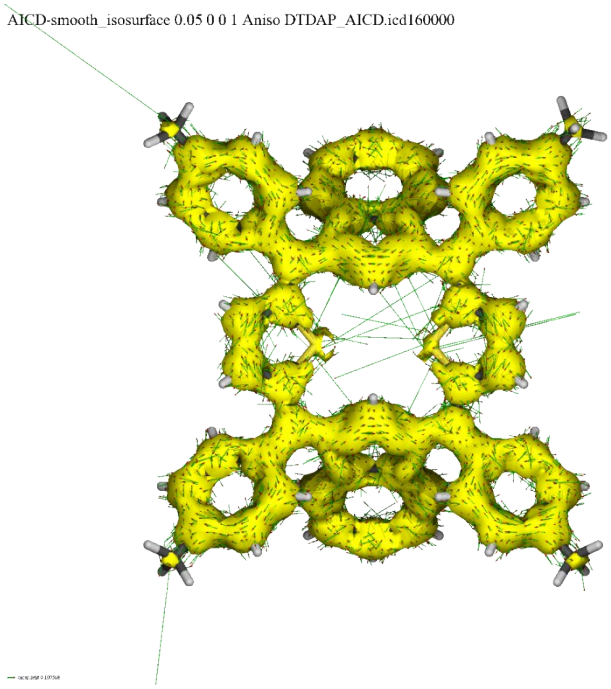

Figure S9. The ACID plots of neutral dithiadiazuliporphyrin (isosurface valuce=0.05)

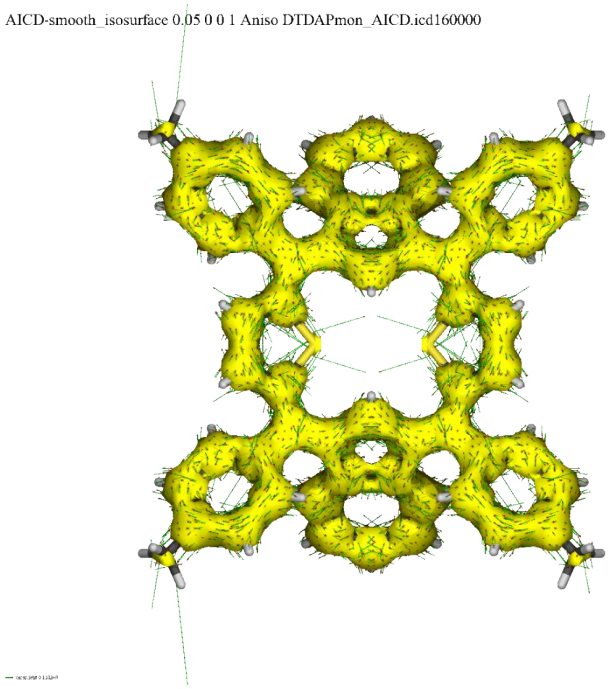

Figure S10. The ACID plots of monocation radical of dithiadiazuliporphyrin (isosurface valuce=0.05)

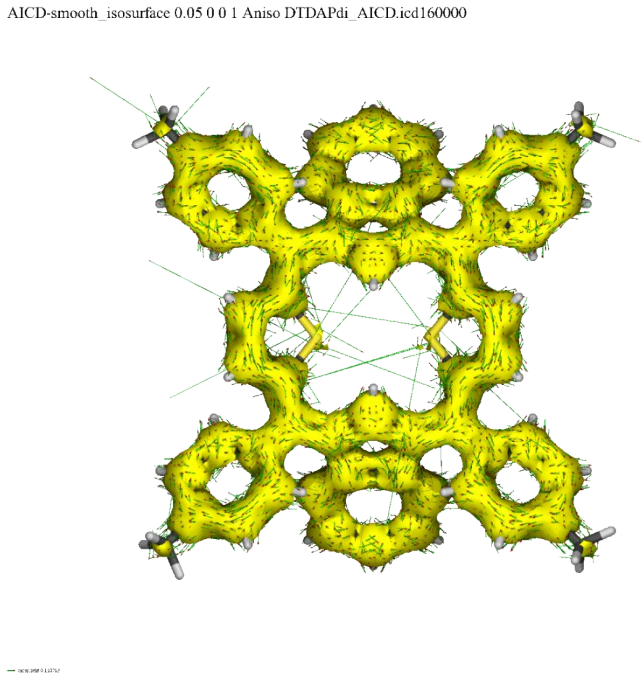

Figure S11. The ACID plots of dication of dithiadiazuliporphyrin (isosurface valuce=0.05)

Table S1. The HOMA, MPD, and NICS(0) value of a series of dithiadiazuliporphyrin

		neutral	monocation	dication
Aromaticity Index	HOMA	0.301	0.556	0.698
	MPD	0.624	0.601	0.607
	NICS(0)	0.415	-2.881	-6.592

Table S2. TD-DFT (B3LYP/6-31G(d,p)) calculated energies, oscillator strengths and compositions of the major electronic transitions of neutral dithiadiazuliporphyrin

Wavelength (nm)	Osc. Strength	Major contribs
821.41	0	HOMO->LUMO (90%)
792.38	1.00E-04	HOMO->L+2 (97%)
738.39	0	HOMO->L+1 (91%)
639.81	0.2401	H-1->LUMO (14%), HOMO->L+3 (79%)
564.56	0.0214	H-1->LUMO (70%), H-1->L+1 (24%)
557.86	9.00E-04	H-1->L+2 (92%)
540.19	0	H-1->L+3 (98%)
483.14	0.0356	HOMO->L+4 (85%)
483.01	1.3959	H-1->LUMO (15%), H-1->L+1 (63%), HOMO->L+3 (17%)
453.65	0.0041	H-2->LUMO (83%)
446.80	0	H-2->L+2 (85%)
446.38	0.1986	HOMO->L+5 (91%)
429.39	0.0154	H-2->L+1 (58%), H-1->L+4 (35%)
401.20	0.2728	H-2->L+1 (35%), H-1->L+4 (60%)
400.11	0.1083	H-2->L+3 (86%)
377.25	0	H-3->L+1 (10%), H-1->L+5 (86%)
371.27	0.0052	HOMO->L+6 (93%)
365.50	0	H-3->LUMO (85%), H-2->L+2 (11%)
362.13	0.0059	HOMO->L+7 (92%)
360.52	0.0175	H-3->L+2 (85%)

Table S3. TD-DFT (B3LYP/6-31G(d,p)) calculated energies, oscillator strengths and compositions of the major electronic transitions of monocation radical of dithiadiazuliporphyrin

Wavelength (nm)	Osc. Strength	Major contribs
1658.42	0.0986	HOMO(B)->LUMO(B) (99%)
1083.68	0	HOMO(A)->L+1(A) (71%), HOMO(A)->L+2(A) (10%)
1075.96	0.0548	H-1(A)->L+1(A) (10%), HOMO(A)->LUMO(A) (43%), HOMO(B)->L+3(B) (38%)
942.70	0	HOMO(A)->L+1(A) (11%), HOMO(A)->L+2(A) (85%)
907.37	0.0001	HOMO(A)->L+3(A) (96%)
887.37	0.0015	HOMO(A)->LUMO(A) (15%), H-1(B)->LUMO(B) (56%), HOMO(B)->L+3(B) (20%)
734.24	0.0116	HOMO(B)->L+1(B) (81%)
708.27	0.0011	HOMO(B)->L+2(B) (83%)
681.04	0.11	H-1(A)->L+1(A) (40%), HOMO(A)->LUMO(A) (21%), H-1(B)->LUMO(B) (25%)
673.38	0	H-1(A)->LUMO(A) (41%), HOMO(A)->L+1(A) (16%), HOMO(B)->L+4(B) (38%)
636.43	0.0004	H-1(A)->L+3(A) (10%), HOMO(A)->L+4(A) (38%), H-2(B)->LUMO(B) (25%)
610.27	0.0024	H-1(A)->L+2(A) (82%)
600.96	0.002	H-1(A)->L+3(A) (56%), H-2(B)->LUMO(B) (36%)
593.48	0	H-1(A)->LUMO(A) (48%), HOMO(B)->L+4(B) (50%)
545.75	0.0481	H-1(A)->L+3(A) (19%), HOMO(A)->L+4(A) (36%), H-2(B)->LUMO(B) (34%)
527.86	0.5766	H-1(A)->L+1(A) (20%), H-4(B)->LUMO(B) (41%), HOMO(B)->L+3(B) (21%)
516.51	0	H-3(B)->LUMO(B) (96%)
513.18	0.0426	H-5(B)->LUMO(B) (85%)
510.81	0.6227	H-1(A)->L+1(A) (23%), HOMO(A)->L+5(A) (18%), H-4(B)->LUMO(B) (32%)
504.59	0.0107	H-1(B)->L+1(B) (67%)

Table S4. TD-DFT (B3LYP/6-31G(d,p)) calculated energies, oscillator strengths and compositions of the major electronic transitions of dication of dithiadiazuliporphyrin

Wavelength (nm)	Osc. Strength	Major contribs
1265.01	0.1877	HOMO->LUMO (102%)
750.64	0.0072	HOMO->L+1 (74%), HOMO->L+2 (19%)
718.83	0.0038	HOMO->L+3 (98%)
696.14	0.0333	H-1->LUMO (27%), HOMO->L+2 (63%)
660.86	0	HOMO->L+4 (98%)
556.58	0.0504	H-2->LUMO (98%)
554.59	0.1451	H-3->LUMO (48%), H-1->LUMO (38%)
544.10	0.0001	H-4->LUMO (89%)
515.48	1.5546	H-3->LUMO (40%), H-1->LUMO (26%), HOMO->L+1 (13%), HOMO->L+2 (14%)
509.65	0.0952	H-5->LUMO (93%)
491.12	0.0021	H-6->LUMO (99%)
488.26	0.0003	H-7->LUMO (94%)
486.69	0.0162	H-9->LUMO (94%)
484.50	0.148	H-8->LUMO (88%)
480.78	0.0056	H-1->L+2 (25%), HOMO->L+5 (72%)
463.92	0.0186	H-1->L+1 (41%), H-1->L+3 (29%)
463.78	0.0123	H-1->L+1 (27%), H-1->L+3 (43%)
424.03	0	H-11->LUMO (85%)
419.10	0.425	H-13->LUMO (13%), H-1->L+1 (13%), H-1->L+2 (51%), HOMO->L+5 (16%)
402.88	0	H-3->L+3 (16%), H-2->L+1 (65%), H-1->L+3 (12%)